

CHAPTER 2

LITERATURE REVIEW

2.1 INTRODUCTION

In this chapter, the basic theory of the nitrogen laser will be reviewed. At the next section, the electrical pumping scheme for this laser, together with the breakdown process, will be discussed. The principles of the previous models of the nitrogen laser will be highlighted too.

2.2 NITROGEN LASER

Nitrogen laser is one of the most common gas lasers and this laser is based on a three-level pumping scheme.

According to the Franck-Condon principle, population inversion in nitrogen laser is obtained by direct impact ionization collisions with molecules from the ground state. The three-level pumping scheme is shown in Fig(2.1). Here, the vibrational and rotational splitting of these three levels are omitted for simplicity.

In this case, population inversion occurs between the $C^3\Pi_u$ and $B^3\Pi_g$ electronic states with an induced emission at a wavelength of 337.1 nm, primarily by the stimulated emission process. Since $C^3\Pi_u$ is a state where its lifetime is about 40ns and $B^3\Pi_g$ is metastable state with a lifetime of about 10 μ s, the population inversion ought to be induced

by a very fast electrical discharge in which the electron density is above 10^{14} cm^{-3} and the electrical current of the discharge is large, in order to avoid the depopulation by spontaneous emission. Therefore, to satisfy these constraints, the nitrogen laser must be operated in the pulse mode. The full width at half maximum (FWHM) of the laser pulse corresponding to the following reaction $C^3\Pi_u \rightarrow B^3\Pi_g$ is very short (about 8 ns)

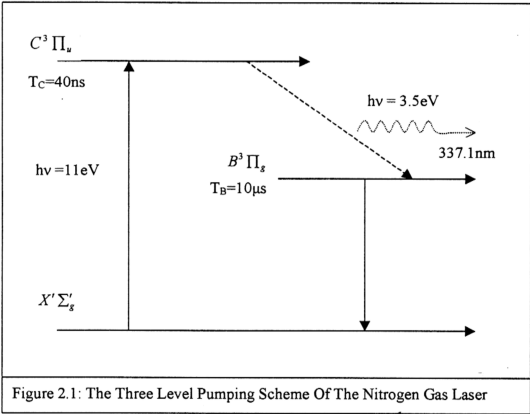


Figure 2.1: The Three Level Pumping Scheme Of The Nitrogen Gas Laser

2.3 FAST ELECTRICAL DISCHARGE PUMPING METHOD

Since the nitrogen laser requires a fast pumping method, the selection of a pumping method will become a major factor that needs to be considered. A good pumping method can ensure a high efficiency optical output.

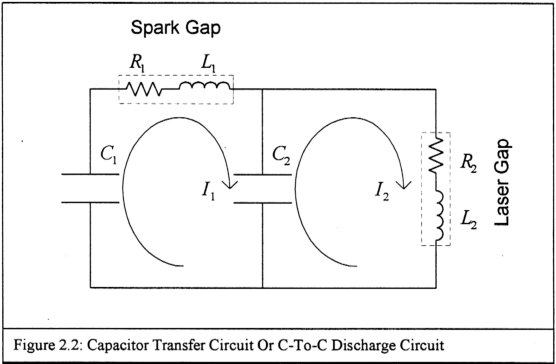
There are many types of pumping methods and the most common and practical is to apply a high voltage electrical discharge. The electrical discharge should also be fast enough to transfer the energy into the gas medium. In order to fulfill the above conditions, two major electrical circuit configurations have been investigated in the previous works (Fitzsimmons, 1976; Spyrou, 1991, 1996). These are the Blumlein circuit and the capacitor transfer circuit. Only the capacitor transfer circuit, or also called as the C-to-C circuit, will be used in this study.

2.3.1 CAPACITOR TRANSFER CIRCUIT

The capacitor transfer circuit is one of the most common pumping methods for gas lasers. The circuit is shown in the Fig(2.2). This discharge circuit is characterized by a very low inductance, a very fast rise time of voltage and current, and also high peak currents.

The C-to-C discharge circuit consists of two major loops, i.e. the charging loop and the discharge loop. A spark gap is situated in the charging loop. When the spark gap is triggered, it will breakdown and ground the storage capacitor, C_1 . All the charge stored in the charging capacitor will then be transferred to the peaking capacitor, C_2 , in a very short period of time. The resistance, R_1 , and inductance, L_1 , of the spark gap should be maintained at a low value in order to reduce the energy lost during the charging process. Voltage of opposite polarity would appear instantaneously on the other plate of the storage capacitor and the peaking capacitor will be charged.

This process will continue until the voltage of the peaking capacitor causes the laser channel to breakdown. The electrical discharge then occurs and the peaking capacitor will dump its energy into the laser channel. The electrons in the gas are accelerated and collide with the gas molecules, creating the population inversion inside the gas medium.



All the charging and discharge processes should not take longer than 40ns to maintain the high efficiency of the laser output.

2.4 ELECTRICAL BREAKDOWN IN GASEOUS MEDIUM

The electrical breakdown of gases has been studied in the laboratory since before the beginning of the twentieth century. Since J. S. Townsend wrote his monograph “The Theory of Ionization of Gases by Collision” (Townsend, 1910), this subject has been widely studied and great progress has been achieved in understanding the problems of electrical breakdown.

From the experiments carried out by Townsend, the importance of the parameter E/p is emphasized, where E is the electrical field and p is the gas pressure. The parameter α is also introduced, which became known as the Townsend Ionization coefficient or the Townsend Primary Coefficient.

2.4.1 TOWNSEND BREAKDOWN MECHANISM

The Townsend or Paschen breakdown mechanism is characterized by a large number of successive electron avalanches that originate from secondary electron generation (Townsend, 1910). It can also explain why a large value of electron current I in a parallel plate discharge gap increased faster than that predicted by the simple exponential law

$$n = n_0 \exp(\alpha d) \quad 2.4.1$$

At the cathode surface, an exponential increase of the electron current within the discharge gap is assumed. The electron current is based on the positive feedback of the Townsend avalanche process through secondary electron emission. This is because Townsend also considered the ionization produced in the gas by positive ions. The equation derived was

$$n = \frac{n_0 \exp(\alpha d)}{1 - (\omega/\alpha)\{\exp(\alpha d)\}} \quad 2.4.2$$

where ω is the generalized secondary ionization coefficient. It includes the action of positive ions, photons and metastable atoms at the cathode. Different secondary processes may dominate under different experimental conditions.

The space charge field caused by differences in the motions between the charges and the positive ions is assumed to be so weak as to be completely negligible. The validity of this assumption will be investigated in this study.

2.4.2 FIRST AND SECOND TOWNSEND COEFFICIENTS

The overall discharge is assumed to be a self sustained discharge. A corresponding equation to the above condition is written as given below (Townsend, 1910)

$$\left(\frac{\alpha}{p}\right)pd = \log \left[\frac{1+\gamma}{\gamma} \right] \quad 2.4.3$$

where p is the gas pressure, d is the electrode gap. Here, α is the first Townsend coefficient. This coefficient measures the exponential rate of production of free electrons per unit mean drift distance of the electrons under the influence of the constant applied electric field strength E under consideration.

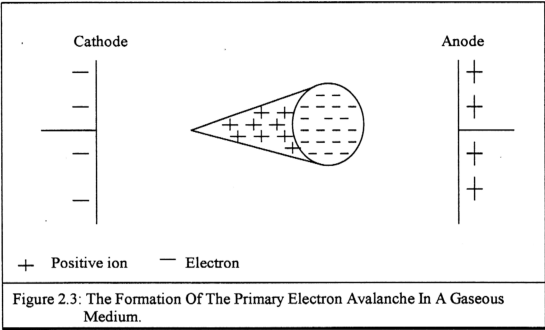
The coefficient γ is the second Townsend coefficient. This coefficient measures the total probability of secondary electron emission from all sources associated with a single primary electron emission. Two major sources contribute to this secondary electron production, i.e. the ion bombardment at the cathode surface and the photoelectric effects. However, only the ion bombardment at the cathode surface will be included in this study since it is the more dominant effect (Fletcher and Blevin, 1981).

2.4.3 SPACE CHARGE EFFECT AND PLASMA STREAMER FORMATION

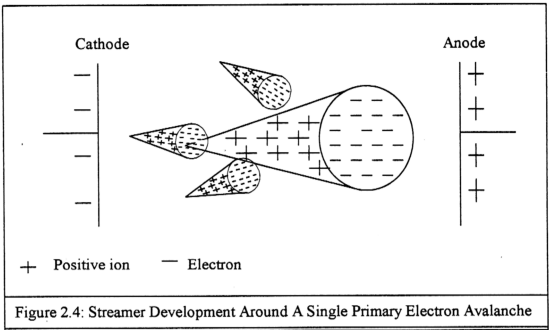
Although the Townsend model describes the breakdown phenomenon in the gas discharge, however, it is still not a complete model. Experimental studies have shown that population inversion is optimal when the high voltage circuit parameters and those of the electrical discharge are also optimized (Persephonis *et al.*, 1993, 1995a, 1995b, 1998). From these previous models, it seems that the best results are obtained when a uniform plasma discharge is formed. However, it is very difficult to maintain this state in reality. The space charge effect will still occur in the gas discharge due to the relatively large difference in velocities of the positive ions and the electrons. Consideration of the space charge effect is needed if the study is carried out for the non-uniform electrical field.

In a fast and short duration pulsed discharge, the electrons are free to move towards the anode. Moreover, the ions are essentially frozen in space in the discharge region. This will result in a primary electron avalanche where the electrons are propagating towards the

to anode and the positive ions are left behind. The formation of the primary electron avalanche is shown in Fig(2.3).



The free electrons are idealized as negatively charged spheres. The shape of the avalanche cone is determined primarily by electron diffusion (Levatter and Lin, 1980). This can cause a space charge effect in the discharge region. At the critical condition where this particular space charge is comparable to the applied electrical field E , the formation of the streamers will begin as shown in Fig(2.4). These streamers develop around a single primary electron avalanche after its space charge field has grown beyond a certain critical value. Amplification of this effect influences the transient behavior of the discharge by increasing the discharge current and initiating processes that cancel the uniform discharge behavior.



The total effect of the streamer formation will lead to the formation of a positively charged layer. This space charge layer will finally form near the cathode, called the cathode sheath.

2.4.4 CATHODE SHEATH FORMATION

The cathode sheath is defined as the region between the cathode and the point where the significant positive net charge density located. Since the electrons are not easily emitted from the cathode and depend on secondary emission properties, the sheath will remain as a space charge layer until there is significant electron production. Therefore, a net positive charge density will exist in the region near the cathode.

The cathode sheath acts as a air capacitor and will be able to hold the charges. This cathode sheath will subsequently collapse if there are a significant numbers of secondary electrons emitted from the cathode due to the ion bombardment process. Once the sheath

collapses, the charges will be free to move and the gap becomes fully conductive. This will lead to electrical breakdown between the electrodes.

2.5 MODELING THE PLASMA IN THE GAS DISCHARGE

In this section, discussions will be focused on earlier studies of the plasma in nitrogen gas discharge. In these previous models (Persephonis *et al.*, 1993, 1995a, 1995b, 1998), the plasma is parameterized by an inductive and resistive elements.

2.5.1 PLASMA WITH RESISTIVE AND INDUCTIVE EFFECTS

A comprehensive theoretical investigation of the performance of a pulsed nitrogen laser is realized through the time-dependent resistances and inductances. According to this method, the waveforms from the electrical discharge are digitized and their first and second derivatives are calculated. The behavior of the plasma can be represented as difference equations and the relationships between the resistances and inductances are formed and calculated for every time step.

Thus, the differential equations for the C-to-C discharge circuit can be written mathematically as given below.

$$L_1 \frac{dI_1}{dt} = -R_1 I_1 - \left(\frac{1}{C_1} + \frac{1}{C_2} \right) \int I_1 dt + \frac{1}{C_2} \int I_2 dt \quad 2.5.1a$$

$$L_2 \frac{dI_2}{dt} = -I_2 R_2 + \frac{1}{C_2} \int I_1 dt - \frac{1}{C_2} \int I_2 dt \quad 2.5.1b$$

where L_2 and R_2 is the inductance and resistance of the discharge gap, respectively. In these circuit equations, the resistance and inductance of the plasma discharge medium are included. These circuit equations can be easily solved numerically.

2.5.2 THE RESISTANCE OF THE DISCHARGE UNDER UNIFORM ELECTRICAL DISCHARGE

Although the plasma can be modeled via the resistive and inductive terms of the circuit equations, it is very difficult to describe these resistive and inductive effects from first principles.

The lack of the knowledge of these time dependent parameters complicates the characterization of the plasma column.

Various assumptions have been made at the previous studies. Many authors initially assumed these inductances and resistances to be constant values (Papadopoulos, 1990, 1991; Iwasaki, 1982). Other authors have assumed the inductance to be constant while the resistance was parameterized through an exponential drop during the formation phase of the discharge, as (Dipace, 1987; Leo, 1991). Here,

$$R = R_0 + R_1 e^{-(t/\tau)} \quad 2.5.2$$

where

$$\tau = \frac{1}{\alpha u_d} \quad 2.5.3$$

α is the first Townsend coefficient and u_d is the drift velocity.

The calculation of the resistance through electron avalanche multiplication, which was carried out by Fitzsimmons (1976), was different from the method above. The new method introduce the resistance of the discharge gap as below

$$R = \frac{d}{S \cdot W \sigma} \quad 2.5.4$$

where, σ is the time-dependent conductivity of the gas given by

$$\sigma = \frac{en_e u_e}{E} \quad 2.5.5$$

Here,

d =Electrode separation

S =Thickness of the arc

W =Active length of the laser tube

E =Electrical field

The resistance of the discharge gap is

$$R = \frac{l}{\mu n e a b}, \quad 2.5.6$$

where

μ =Electron mobility

n =Electron number density

e =Electron charge

l =Interelectrode distance

a =Length of the discharge volume

b =Thickness of the discharge volume

However, this method can only be applied when the electrical field is assumed to be uniform. In order to get a clearer and more realistic picture of the electrical discharge of nitrogen gas, it is necessary to study the non-uniform electrical field. For a further investigation of the gaseous discharge under different configurations, a new model needs to be built up. In this new model, the fluid behavior of the plasma is simulated.

2.6 THE FLUID BEHAVIOR OF THE PLASMA

The plasma in a gaseous discharge can be described as a fluid. At the initial stage of the discharge, the ions and electrons are free to move in the discharge medium under the

Here,

d =Electrode separation

S =Thickness of the arc

W =Active length of the laser tube

E =Electrical field

The resistance of the discharge gap is

$$R = \frac{l}{\mu neab}, \quad 2.5.6$$

where

μ =Electron mobility

n =Electron number density

e =Electron charge

l =Interelectrode distance

a =Length of the discharge volume

b =Thickness of the discharge volume

However, this method can only be applied when the electrical field is assumed to be uniform. In order to get a clearer and more realistic picture of the electrical discharge of nitrogen gas, it is necessary to study the non-uniform electrical field. For a further investigation of the gaseous discharge under different configurations, a new model needs to be built up. In this new model, the fluid behavior of the plasma is simulated.

2.6 THE FLUID BEHAVIOR OF THE PLASMA

The plasma in a gaseous discharge can be described as a fluid. At the initial stage of the discharge, the ions and electrons are free to move in the discharge medium under the

influence of the external electrical field. This process will continue until the space charge field has grown sufficiently to affect the motion of the charged particles.

2.6.1 CONTINUITY EQUATIONS IN PHYSICS

The fluid behavior of the plasma in gaseous discharge can be represented by the continuity equations. In order to model the motion of the charged particles with its velocities, V , and its densities, ρ , in the particular discharge, a continuity equation in partial differential form is required. The clear picture on the distributions of these particles can be seen, specially its distributions in a non-uniform electrical field. However, solving the continuity is not easy due to its numerical stability and accuracy requirement.

The ordinary continuity equation can be written as below:

$$\frac{\partial \rho}{\partial t} + V \cdot \nabla \rho = -\rho \nabla \cdot V \quad 2.6.1a$$

or in conservative form

$$\frac{\partial \rho}{\partial t} = -\nabla \cdot \rho V \quad 2.6.1b$$

These equations are used to describe two phenomena taking place simultaneously, i.e. convection and compression. Compression is described by the $\rho \nabla \cdot V$ term. This term does not really pose as many numerical difficulties as convection, i.e., propagation along the characteristics. However, the convective term, $V \cdot \nabla \rho$ in Eq(2.6.1a), makes this equation one of the most difficult partial differential equations of continuum physics to be solved with stability and accuracy.

Numerically solving the continuity equations requires some powerful algorithms. In this study, a finite-difference algorithm, the Flux-Corrected Transport (FCT), is chosen.

The FCT techniques are capable of solving these continuity equations more accurately and reliably than straightforward mathematical expansion alone.

2.6.2 REQUIREMENT FOR FINITE-DIFFERENCE ALGORITHMS

Over the years, many schemes have been attempted to improve numerical solutions of continuity equations. These include the method of characteristics, spectral methods, finite-element methods, splines, and finite-difference methods.

Characteristic methods and spectral methods are not generally applicable to complicated nonlinear systems of continuity equations, while giving superb results in some cases, such as the diffusion effects as well as convection and compression.

Finite-element and spline approaches also give excellent results in most cases. However, these methods are complex and their computational costs are often prohibitively high.

Thus, the attention naturally turns time and again to the simple, generally applicable, computationally efficient, finite-difference formulations.

Since the finite-difference algorithms are generally simple and fast, the improvement of the basic finite-difference schemes needs to be more accurate without sacrificing too much of their simplicity or speed. These basic ideas led to the development of a new scheme of algorithms by Boris and Book (1973, 1975, 1976a, 1976b), and are designed to satisfy a set of seven requirements listed as follows:

1. Exact conservation properties of the physical equation should be mirrored in the finite-difference approximations.
2. The algorithm should ensure stability of all the harmonics in some useful range of the grid spacing δx and the time-step δt .

3. The positivity (nonnegativity) property of $\rho(x, t)$ in continuity equation as in Eq(2.6.1) should be preserved. Thus, if the density ρ is positive and decreasing (in time), it stops changing as it approaches zero density.
4. The algorithm should not be built around special properties such as giving exactly the correct answer when $V \partial \rho / \partial x = 1$.
5. The overall algorithm should be effectively second order in regions of the problem where the concept of order is related usefully to accuracy. This requirement is included to provide a minimal long-term accuracy free of at least the worst types of secularity.
6. The algorithm should leave the numerical density profile ρ undisturbed when the flow velocity is zero.
7. The algorithm should have a single or double step time integration to ensure simple, fast, efficient calculations.

The first three requirements govern the conservation, stability, and positivity of the algorithm, and the last four requirements referred to the concepts concerning flexibility and accuracy. This new algorithm is called the Flux-Corrected Transport (FCT).

2.6.3 THE PRINCIPLES OF FLUX-CORRECTED TRANSPORT (FCT) ALGORITHM

In this study, the Flux-Corrected Transport is used to solve the fluid equations. Previous researchers had proven that this method provides a powerful numerical algorithm to solve these equations with high stability and accuracy (Boris and Book, 1973, 1975, 1976a, 1976b; Morrow, 1981).

2.6.3.1 INTRODUCTION

The Flux-Corrected Transport (FCT) algorithm was first introduced by Boris and Book (1973). These flux-corrected transport algorithms are of indeterminate order but yield realistic accurate results. In addition to the mass-conserving property of most conventional algorithms, the FCT algorithm strictly maintains the positivity of actual mass densities. Steep gradients and inviscid shocks are thus handled particularly well.

2.6.3.2 POSITIVITY AND ACCURACY

Positivity is a property satisfied by the continuity equation, i.e. the density $\rho(x, t)$ in Eq(2.6.1) is everywhere positive and the source terms are zero. It is a mathematical consequence of the continuity equation and an obvious physical property of the flow that the density can never assume negative values.

In order to retain these physical and mathematical properties into difference equations, such as Eulerian algorithms, a certain amount of numerical diffusion need to be included. This numerical diffusion has the consequence that the solution remains stable while retaining positivity.

Numerical diffusion is an inherent problem. It can invalidate numerical calculations and reduce the accuracy while using linear algorithms, unless they have very fine computational meshes are used.

The continuity equation, Eq(2.6.1), can also be considered as a three point explicit finite-difference formula as below:

$$\rho_i^{n+1} = a_i \rho_{i-1}^n + b_i \rho_i^n + c_i \rho_{i+1}^n \quad 2.6.2$$

where ρ_i^{n+1} is one time step further than ρ_i^n .

This general form includes the first-order upwind algorithm and other common algorithms. If Δx and Δt are constants, Eq(2.6.2) can be rewritten in a form that guarantees conservation,

$$\rho_i^{n+1} = \rho_i^n - \frac{1}{2} \left(\varepsilon_{i+\frac{1}{2}} (\rho_{i+1}^n + \rho_i^n) - \varepsilon_{i-\frac{1}{2}} (\rho_i^n + \rho_{i-1}^n) \right) + \left(v_{i+\frac{1}{2}} (\rho_{i+1}^n + \rho_i^n) - v_{i-\frac{1}{2}} (\rho_i^n + \rho_{i-1}^n) \right) \quad 2.6.3$$

The convective coefficients $\varepsilon_{i\pm\frac{1}{2}}$ are given as:

$$\varepsilon_{i\pm\frac{1}{2}} = v_{i\pm\frac{1}{2}} \frac{\Delta t}{\Delta x} \quad 2.6.4$$

where $v_{i\pm\frac{1}{2}}$ are the velocities.

The $v_{i\pm\frac{1}{2}}$ are the nondimensional numerical diffusion coefficients which appear as a consequence of considering adjacent grid points. Conservation of ρ in Eq(2.6.3) also constrains the coefficients a_i , b_i and c_i by the condition:

$$a_{i+1} + b_i + c_{i-1} = 1 \quad 2.6.5$$

Positivity of ρ_i^{n+1} for all possible positive profiles ρ_i^n requires that a_i , b_i and c_i be positive for all i . By matching the corresponding terms and the condition in Eqs(2.6.2) and (2.6.3), we will get

$$a_i = v_{i-\frac{1}{2}} + \frac{1}{2} \varepsilon_{i-\frac{1}{2}} \quad 2.6.6a$$

$$b_i = 1 - \frac{1}{2} \varepsilon_{i+\frac{1}{2}} + \frac{1}{2} \varepsilon_{i-\frac{1}{2}} - v_{i+\frac{1}{2}} - v_{i-\frac{1}{2}} \quad 2.6.6b$$

$$c_i = v_{i+\frac{1}{2}} - \frac{1}{2} \varepsilon_{i+\frac{1}{2}} \quad 2.6.6c$$

In order to ensure ρ_i^{n+1} to be always positive, $v_{i+\frac{1}{2}}$ needs to be positive and sufficiently large. The positivity conditions derived from Eqs(2.6.6) are,

$$|\varepsilon_{i+\frac{1}{2}}| \leq \frac{1}{2} \quad 2.6.7a$$

$$\frac{1}{2}|\varepsilon_{i+\frac{1}{2}}| \leq v_{i+\frac{1}{2}} \leq \frac{1}{2} \quad \text{for all } i. \quad 2.6.7b$$

If algorithms are used with $\frac{1}{2}|\varepsilon_{i+\frac{1}{2}}| > v_{i+\frac{1}{2}}$, positivity is not necessarily destroyed but can no longer be guaranteed. The diffusion coefficient $v_{i+\frac{1}{2}}$ cannot be zero, due to the explicit three points formula in Eq(2.6.3). The numerical stability problem will occur if this value is zero.

The condition in Eq(2.6.7) for positivity leads directly to numerical diffusion in addition to the desired convection:

$$\rho_i^{n+1} = \rho_i^n + v_{i+\frac{1}{2}}(\rho_{i+1}^n + \rho_i^n) - v_{i-\frac{1}{2}}(\rho_i^n + \rho_{i-1}^n) + \text{convection} \quad 2.6.8$$

Finite difference methods which are higher than first order, such as the Lax-Wendroff methods, reduce the numerical diffusion but sacrifice assured positivity. This apparent dilemma can only be resolved by using a nonlinear method to integrate the continuity equations.

2.6.4 THE BASIC IDEA OF FLUX-CORRECTED TRANSPORT (FCT)

The basic concepts of Flux-Corrected Transport (FCT) can be derived in a rather straightforward way. Simplicity leads us to start with an explicit three point approximation to the continuity equation.

The FCT algorithm actually consists conceptually of two major stages, a transport or convective stage (Stage 1) followed by an antidiffusive or corrective stage (Stage 2). Both

stages are conservative and maintain positivity. Their interaction enables FCT algorithms to treat strong gradients and shocks without the usual generated ripples.

2.6.4.1 THE TRANSPORT STAGE

The explicit three-point approximation to the continuity equation given by Eq(2.6.2) can be rewritten as below:

$$\tilde{\rho}_i = a_i \rho_{i-1}^o + b_i \rho_i^o + c_i \rho_{i+1}^o \quad 2.6.9$$

This equation is used to determine provisional value, $\tilde{\rho}_i$, from the previous time step or “old” values, ρ_i^o .

The conservation condition at Eq(2.6.5) must be satisfied and the value of a_i , b_i and c_i must all be greater than or equal to zero to assure positivity.

The Eq(2.6.9) in conservation form will become:

$$\begin{aligned} \tilde{\rho}_i &= \rho_i^o - \frac{1}{2} \left(\varepsilon_{i+\frac{1}{2}} (\rho_{i+1}^o + \rho_i^o) - \varepsilon_{i-\frac{1}{2}} (\rho_i^o + \rho_{i-1}^o) \right) + \left(v_{i+\frac{1}{2}} (\rho_{i+1}^o + \rho_i^o) - v_{i-\frac{1}{2}} (\rho_i^o + \rho_{i-1}^o) \right) \\ &= \rho_i^o - \frac{1}{\Delta x} \left[f_{i-\frac{1}{2}} - f_{i+\frac{1}{2}} \right] \end{aligned} \quad 2.6.10$$

The values of variables at interface $i + \frac{1}{2}$ are averages (possibly unequally weighted) of values at cells $i + 1$ and i , and the values at $i - \frac{1}{2}$ are averages of values at cells i and $i - 1$. At every cell i , the $\tilde{\rho}_i$ differs from ρ_i^o as a result of the inflow and out flow fluxes of ρ , denoted by $f_{i\pm\frac{1}{2}}$ across the cell boundaries.

The fluxes are successively added and subtracted along the array of densities ρ_i^o so that the overall conservation of ρ is satisfied by construction. Summing all the provisional

densities gives the sum of the old densities. The expressions involve the convective fluxes, $\varepsilon_{i\pm\frac{1}{2}}$.

The relation between a , b and c coefficients with the ε and ν are essentially discussed as in Eq(2.6.6) in the last section.

The diffusion coefficients, $\nu_{i\pm\frac{1}{2}}$ are included to ensure positivity of the provisional values, $\tilde{\rho}_i$. The positivity condition for this provisional values, $\tilde{\rho}_i$ has been discussed as in Eq(2.6.7).

However, after Eq(2.6.9) is imposed, two of the three coefficients in Eq(2.6.10) still need to be determined. One of these sets of coefficients must ensure an accurate representation of the mass flux terms. Thus

$$\varepsilon_{i+\frac{1}{2}} = \nu_{i+\frac{1}{2}} \frac{\Delta t}{\Delta x} \quad 2.6.11$$

where, $\nu_{i+\frac{1}{2}}$ is the fluid velocity approximated at the cell interfaces. The other set of coefficients, $\nu_{i\pm\frac{1}{2}}$ are chosen to maintain positivity and stability. The choices of $\nu_{i\pm\frac{1}{2}}$ will be discussed at the next section.

2.6.4.2 THE ANTIDIFFUSION STAGE

After the transport stage, the provisional value must be strongly diffused to ensure positivity. For example, if the $\nu_{i+\frac{1}{2}} = \frac{1}{2} \left| \varepsilon_{i+\frac{1}{2}} \right|$ in Eq(2.6.7), we will have the diffusive, first order upwind algorithm. It is the heavily diffusive donor-cell algorithm.

Any other choices for $\nu_{i+\frac{1}{2}}$ can only be more diffusive in order to preserve positivity. The problem will occur since the positivity and accuracy are mutually exclusive. An obvious correction to get around this overstrong diffusion is needed.

In order to remove the strong diffusion elements in the algorithms, an antidiffusion stage has been introduced. In this stage, a correction is being used and the equation is being written as below:

$$\begin{aligned}\rho_i^n &= \tilde{\rho}_i - \mu_{i+\frac{1}{2}}(\tilde{\rho}_{i+1} - \tilde{\rho}_i) + \mu_{i-\frac{1}{2}}(\tilde{\rho}_i - \tilde{\rho}_{i-1}) \quad \text{or} \\ &= \tilde{\rho}_i - f_{i+\frac{1}{2}}^{ad} + f_{i-\frac{1}{2}}^{ad}\end{aligned}\tag{2.6.12}$$

The new value of ρ_i^n is calculated after the positive antidiffusion coefficient $f_{i+\frac{1}{2}}^{ad}$ is added. This antidiffusive factor will reduce the strong diffusion implied by the Eq(2.6.7).

Although the antidiffusion reduces the strong diffusion implied by Eq(2.6.7), it also reintroduces the possibility of negative densities in the new profile $\tilde{\rho}_i$. Instability is even possible if the values $\mu_{i+\frac{1}{2}}$ are too large. In order to avoid this apparent bind, the modification has to be carried out to the antidiffusive fluxes in Eq(2.6.12). This method is called flux correction or flux limiting method. This is due to the antidiffusive fluxes

$$f_{i+\frac{1}{2}}^{ad} \equiv \mu_{i+\frac{1}{2}}(\tilde{\rho}_{i+1} - \tilde{\rho}_i)\tag{2.6.13}$$

appearing in Eq(2.6.12) that have to be corrected or limited to assure positivity as well as stability.

The best linear choice of $f_{i+\frac{1}{2}}^{ad}$ which still retains positivity is given below:

$$\mu_{i+\frac{1}{2}} \approx \nu_{i+\frac{1}{2}} - \frac{1}{2} \left| \epsilon_{i+\frac{1}{2}} \right|\tag{2.6.14}$$

However, this is still not good enough. To reduce the residual diffusion $\mu_{i+\frac{1}{2}} - \nu_{i+\frac{1}{2}}$ further, the flux correction has to be nonlinear. It must depend on the actual values of the density $\tilde{\rho}_i$.

The basic idea of the nonlinear flux correction formula is to create no new maxima or minima in the solution. For example, the density $\tilde{\rho}_i$ at grid point i reaches zero sooner than its neighbors. Then the second derivative is locally positive and so any finite antidiffusion would force the minimum density value $\tilde{\rho}_i = 0$ to become negative. Since this condition will not happen physically, the antidiffusive fluxes should be limited so that minima in the profile can be made and the value is no deeper than the antidiffusive stage defined by Eq. (2.6.12). In this manner, the maxima in the profile must be made lower than the antidiffusion terms.

Combining the two condition above, it will form the basis of the Flux Corrected-Transport method:

The antidiffusion stage should generate no new maxima or minima in the solution, nor should it accentuate already existing extrema.

This qualitative formulation for nonlinear filtering can be quantified easily. The new flux-corrected transport values ρ_i^n are given by

$$\rho_i^n = \tilde{\rho}_i - f_{i+\frac{1}{2}}^c + f_{i-\frac{1}{2}}^c \quad 2.6.15$$

where the corrected fluxes $f_{i+\frac{1}{2}}^c$ should satisfy

$$f_{i+\frac{1}{2}}^c \equiv S \cdot \max \left\{ 0, \min \left[S \cdot (\tilde{\rho}_{i+2} - \tilde{\rho}_{i+1}), \left| f_{i+\frac{1}{2}}^{ad} \right|, S \cdot (\tilde{\rho}_i - \tilde{\rho}_{i-1}) \right] \right\} \quad 2.6.16$$

Here $|S| = 1$ and $\text{sign } S \equiv \text{sign}(\tilde{\rho}_{i+2} - \tilde{\rho}_{i+1})$.

In order to know what this flux-correction formula is doing, assume that $(\tilde{\rho}_{i+2} - \tilde{\rho}_{i+1})$ is greater than zero. Then the Eq(2.6.16) will become:

$$f_{i+\frac{1}{2}}^c = \min \left[(\tilde{\rho}_{i+2} - \tilde{\rho}_{i+1}), \mu_{i+\frac{1}{2}} (\tilde{\rho}_{i+1} - \tilde{\rho}_i), (\tilde{\rho}_i - \tilde{\rho}_{i-1}) \right] \quad 2.6.17a$$

or

$$f_{i+\frac{1}{2}}^c = 0 \quad 2.6.17b$$

The "raw" antidiffusive flux $f_{i+\frac{1}{2}}^{ad} \equiv \mu_{i+\frac{1}{2}} (\tilde{\rho}_{i+1} - \tilde{\rho}_i)$ always tends to decrease ρ_i^n and to increase ρ_{i+1}^n . The flux-limiting formula only ensures that the corrected flux cannot push ρ_i^n below ρ_{i-1}^n (which would be a new minimum) nor push ρ_{i+1}^n above ρ_{i+2}^n (which would give a new maximum). The general formula Eq(2.6.16) is being constructed to take care of all cases of sign and slope.

2.7 DISCHARGE CURRENT INDUCED BY THE MOTION OF THE CHARGED PARTICLES

From the literature, a formula for the discharge current is derived for a general electrode geometry from the energy balance equation in which the displacement current is explicitly taken into account (Sato, 1980).

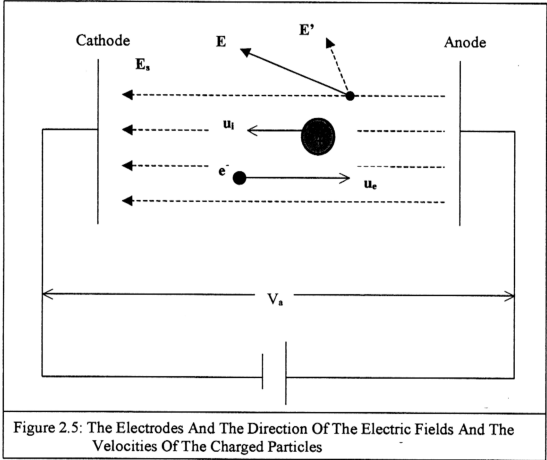
From Fig(2.5), the schematic diagram shows the geometry of the electrodes, the direction of the electric fields and the drift velocities of the charged particles.

The V_a and I are the constant applied potential and the current in the external circuit. The space charge distributions in the gap are represented by the continuity equations for electrons and ions as below:

$$\frac{\partial n_i}{\partial t} + \nabla \cdot (n_i \mathbf{u}_i) = \alpha n_i |\mathbf{u}_e| \quad 2.7.1a$$

$$\frac{\partial n_e}{\partial t} + \nabla \cdot (n_e \mathbf{u}_e) = \alpha n_e |\mathbf{u}_e| \quad 2.7.1b$$

where α is the electron ionization coefficient in the discharge medium. n and u are the number densities and velocities of the charged carriers. i and e correspond to the positive ions and the electrons. Combination of these two equations, we can get the net charge density ρ as below



$$\frac{\partial \rho}{\partial t} = e \nabla \cdot (n_i \mathbf{u}_i - n_e \mathbf{u}_e)$$

$$e \frac{\partial (n_i - n_e)}{\partial t} = e \nabla \cdot (n_i \mathbf{u}_i - n_e \mathbf{u}_e) \quad 2.7.2$$

The electric field in the discharge medium is also being modified by the space charge

$$\mathbf{E} = \mathbf{E}_s + \mathbf{E}' \quad 2.7.3$$

where \mathbf{E}_s is the static applied electrical field and \mathbf{E}' is the field produced by the space charge. Since the static applied electrical field is always uniformly distributed in the discharge medium and the space charge field depends on the net charged densities in the gaseous medium, we can list down some general relations as written as below

$$\nabla \cdot \mathbf{E}_s = 0 \quad 2.7.4a$$

$$\nabla \cdot \mathbf{E}' = \frac{\rho}{\epsilon_0} \quad 2.7.4b$$

and

$$\mathbf{E}' = -\nabla \psi \quad 2.7.4c$$

where ψ is the potential of the field caused by the space charge.

From the energy balance equation containing the displacement current

$$V_s I = \int_V e(n_i \mathbf{u}_i - n_e \mathbf{u}_e) \cdot \mathbf{E} dv + \epsilon_0 \int_V \frac{\partial \mathbf{E}'}{\partial t} \cdot \mathbf{E} dv \quad 2.7.5$$

where $\int_V dv$ represents the volume integration over the discharging space. The second term of the Eq(2.7.5) represents the rate of change of the electric field energy which has been pointed out by Horii (1976) to be take into account in the energy balance equation.

The first term of the equation (2.7.5) can be divided into two terms

$$\int_V e(n_i \mathbf{u}_i - n_e \mathbf{u}_e) \cdot \mathbf{E} dv = \int_V e(n_i \mathbf{u}_i - n_e \mathbf{u}_e) \cdot \mathbf{E}_s dv + \int_V e(n_i \mathbf{u}_i - n_e \mathbf{u}_e) \cdot \mathbf{E}' dv \quad 2.7.6$$

The second term of Eq(2.7.6) can be partially integrated by use of the relation

$\mathbf{E}' = -\nabla \psi$ and becomes

$$\int_V e(n_i \mathbf{u}_i - n_e \mathbf{u}_e) \cdot \mathbf{E}' dv = - \int_S \psi e(n_i \mathbf{u}_i - n_e \mathbf{u}_e) \cdot d\mathbf{S} + \int_V \psi e \nabla \cdot (n_i \mathbf{u}_i - n_e \mathbf{u}_e) dv$$

where $\int_S \mathbf{dS}$ represents the surface integration over the closed surface of the discharging space. The first term of Eq(2.7.7) is zero when the integral is take over the surface of the electrodes and infinitely distant from the gap. The second term of the Eq(2.7.7) can be rewritten by use of Eq(2.7.2) and $\nabla \cdot \mathbf{E}' = \frac{\rho}{\epsilon_o}$ as below

$$\begin{aligned}
 \int_V \psi e \nabla \cdot (n_i \mathbf{u}_i - n_e \mathbf{u}_e) dv &= \int_V \psi \frac{\partial \rho}{\partial t} dv \\
 &= \int_V \epsilon_o \psi \frac{\partial}{\partial t} (\nabla \cdot \mathbf{E}') dv \\
 &= -\epsilon_o \int_S \psi \frac{\partial \mathbf{E}'}{\partial t} \cdot \mathbf{dS} - \epsilon_o \int_V \frac{\partial \mathbf{E}'}{\partial t} \cdot \mathbf{E}' dv \\
 &= \epsilon_o \int_V \frac{\partial \mathbf{E}'}{\partial t} \cdot \mathbf{E}' dv
 \end{aligned} \tag{2.7.8}$$

From the Eq(2.7.5), we now can rewrite it as

$$\begin{aligned}
 V_a I &= \int_V e (n_i \mathbf{u}_i - n_e \mathbf{u}_e) \cdot \mathbf{E} dv + \epsilon_o \int_V \frac{\partial \mathbf{E}'}{\partial t} \cdot \mathbf{E} dv \\
 &= \int_V e (n_i \mathbf{u}_i - n_e \mathbf{u}_e) \cdot \mathbf{E}_s dv + \epsilon_o \int_V \frac{\partial \mathbf{E}'}{\partial t} \cdot \mathbf{E} dv - \epsilon_o \int_V \frac{\partial \mathbf{E}'}{\partial t} \cdot \mathbf{E}' dv \\
 &= \int_V e (n_i \mathbf{u}_i - n_e \mathbf{u}_e) \cdot \mathbf{E}_s dv + \epsilon_o \int_V \frac{\partial \mathbf{E}'}{\partial t} \cdot \mathbf{E}_s dv
 \end{aligned} \tag{2.7.9}$$

due to the Eq(2.7.3)

The partial integration of the second term of Eq(2.7.9) given by

$$\begin{aligned}
 \epsilon_o \int_V \frac{\partial \mathbf{E}'}{\partial t} \cdot \mathbf{E}_s dv &= -\epsilon_o \int_S \frac{\partial \psi}{\partial t} \mathbf{E}_s \cdot \mathbf{dS} + \epsilon_o \int_V \frac{\partial \psi}{\partial t} \nabla \cdot \mathbf{E}_s dv \\
 &= 0
 \end{aligned} \tag{2.7.10}$$

because of the $\nabla \cdot \mathbf{E}_s = 0$

Finally the Eq(2.7.5) will become

$$V_a I = \int_v e(n_i \mathbf{u}_i - n_e \mathbf{u}_e) \cdot \mathbf{E}_s dv \quad 2.7.11$$

Therefore, the formula of the discharge current is

$$I = \frac{e}{V_a} \int_v (n_i \mathbf{u}_i - n_e \mathbf{u}_e) \cdot \mathbf{E}_s dv \quad 2.7.12$$

From this formula, we noticed that the influence of the field produced by space charge does not appear explicitly. It is evident that Eq(2.7.12) is compatible with the principle of superposition.